iScience

CellPress
OPEN ACCESS

Article

Microglial apolipoprotein E particles contribute to neuronal senescence and synaptotoxicity

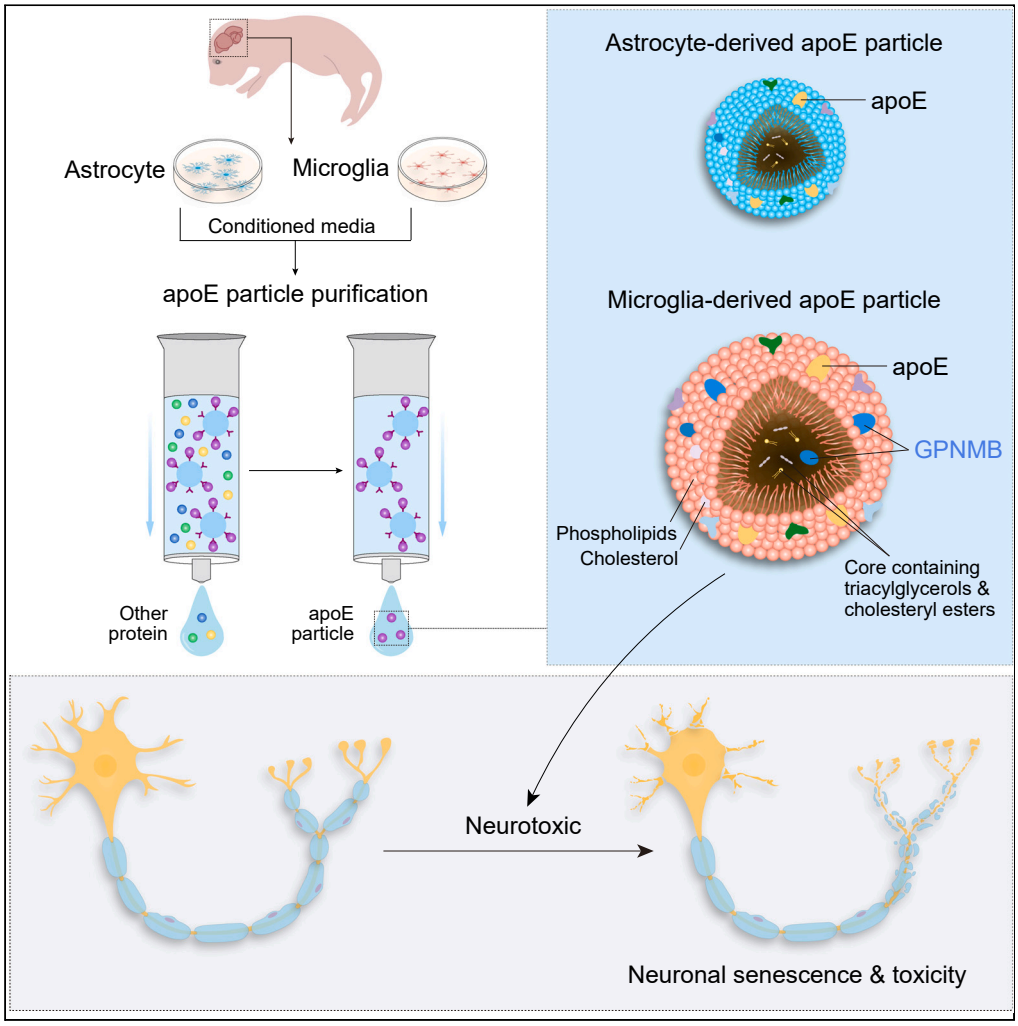

Na Wang, Lujian Cai, Xinyu Pei, ..., Hongsheng Zhang, Yingjun Zhao, Huaxi Xu

wangzx@xmu.edu.cn (Z.W.)
hszhang@cqmu.edu.cn (H.Z.)
yjzhao@xmu.edu.cn (Y.Z.)

Highlights

Microglial apoE particles exhibit larger size than astrocytic apoE particles

Microglial apoE particles are neurotoxic and promote neuronal senescence

GPNMB mediates neuronal toxicity and senescence induced by microglial apoE particles

Microglial APOE4 particles exhibit larger size and more severe neurotoxicity

Wang et al., iScience 27, 110006
June 21, 2024
https://doi.org/10.1016/j.isci.2024.110006

iScience

CellPress
OPEN ACCESS

Article

Microglial apolipoprotein E particles contribute to neuronal senescence and synaptotoxicity

Na Wang,[1,5] Lujian Cai,[1,5] Xinyu Pei,[1] Zhihao Lin,[1] Lihong Huang,[1,2] Chensi Liang,[1] Min Wei,[1] Lin Shao,[1] Tiantian Guo,[1] Fang Huang,[3,4] Hong Luo,[1] Honghua Zheng,[1] Xiao-fen Chen,[1] Lige Leng,[1] Yun-wu Zhang,[1] Xin Wang,[1,2] Jie Zhang,[1] Kai Guo,[3,4] Zhanxiang Wang,[1,*] Hongsheng Zhang,[3,4,*] Yingjun Zhao,[1,7,*] and Huaxi Xu[1,3,6]

SUMMARY

Apolipoprotein E (apoE) plays a crucial role in the pathogenesis of Alzheimer's disease (AD). Microglia exhibit a substantial upregulation of apoE in AD-associated circumstances, despite astrocytes being the primary source of apoE expression and secretion in the brain. Although the role of astrocytic apoE in the brain has been extensively investigated, it remains unclear that whether and how apoE particles generated from astrocytes and microglia differ in biological characteristic and function. Here, we demonstrate the differences in size between apoE particles generated from microglia and astrocytes. Microglial apoE particles impair neurite growth and synapses, and promote neuronal senescence, whereas depletion of GPNMB (glycoprotein non-metastatic melanoma protein B) in microglial apoE particles mitigated these deleterious effects. In addition, human APOE4-expressing microglia are more neurotoxic than APOE3-bearing microglia. For the first time, these results offer concrete evidence that apoE particles produced by microglia are involved in neuronal senescence and toxicity.

INTRODUCTION

Alzheimer's disease (AD) is the most common form of dementia, accounting for around 60–80% of all cases.[1] In addition to extracellular amyloid plaques and intracellular neurofibrillary tangles in the brain,[2–4] emerging evidence demonstrates critical roles of microglia in the pathogenesis of AD.[5–12] Microglia, as the resident brain macrophage, are the primary immune cells within the central nervous system (CNS).[13–15] Physiologically, microglia play an essential role in maintaining normal neuronal functions in the CNS by modulating synaptic activity and eliminating toxic waste.[16–21] Activated microglia display a variety of phenotypes and interact with tau and amyloid-β pathology, contributing in different ways to either promote or inhibit the development of AD.[22–27] Therefore, comprehending the role of microglia and the underlying brain mechanisms may provide new insights into AD treatment approaches.

The apolipoprotein E (apoE) gene (*APOE*) exists as three polymorphic alleles (ε2, ε3, and ε4) in human,[28–30] among which *APOE ε4* is the strongest genetic risk factor for late-onset AD.[2,30–33] Under physiological condition, apoE is produced and secreted primarily by astrocytes in the brain.[34] Secreted apoE is associated with other proteins and lipids in the form of particles.[35,36] Aβ may be sequestered by astrocyte-derived apoE particles, which also display isoform and cell-state-specific lipidation; and this could facilitate cellular uptake and the breakdown of apoE-Aβ complexes.[30,37] Cumulative evidence demonstrates that apoE expression is dramatically increased in microglia under AD-associated pathological conditions.[38] Microglial apoE may regulate AD pathogenesis through the regulation of associated inflammation, lipid transport or the clearance of pathology.[21,25,39–41] However, it has not been fully elucidated whether and how apoE particles derived from microglia and astrocytes differ in biological features and functions.

In this study, we characterized the biological properties of apoE particles from primary microglia and astrocytes. Additionally, we examined the impact of astrocytic and microglial apoE particles on neurons and elucidated the underlying mechanisms.

[1]Center for Brain Sciences, First Affiliated Hospital of Xiamen University, Institute of Neuroscience, Fujian Provincial Key Laboratory of Neurodegenerative Disease and Aging Research, School of Medicine, Xiamen University, Xiamen, Fujian 361005, China
[2]State Key Laboratory of Cellular Stress Biology, Xiamen University, Xiamen 361102, China
[3]Institute for Brain Science and Disease, Chongqing Medical University, Chongqing 400016, China
[4]Key Laboratory of Major Brain Disease and Aging Research (Ministry of Education), Chongqing 400016, China
[5]These authors contributed equally
[6]Deceased
[7]Lead contact
*Correspondence: wangzx@xmu.edu.cn (Z.W.), hszhang@cqmu.edu.cn (H.Z.), yjzhao@xmu.edu.cn (Y.Z.)
https://doi.org/10.1016/j.isci.2024.110006

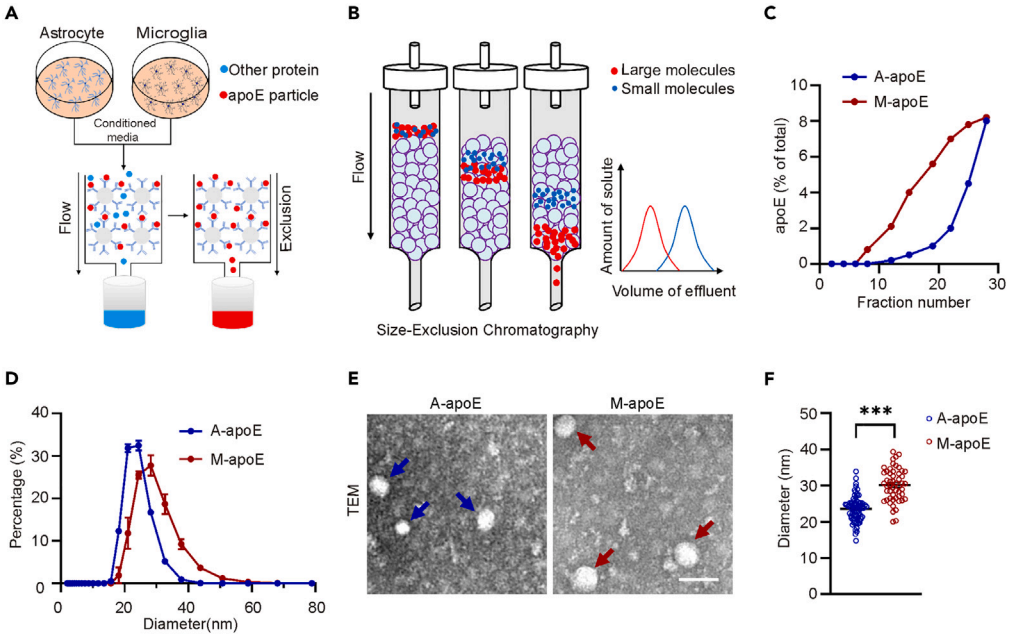

Figure 1. Characterization of apoE particles

(A) Schematic illustration of apoE particle purification by apoE antibody column.

(B) Schematic illustration of apoE particle analysis by size exclusion chromatography (SEC).

(C) ApoE particle ratios in different elution fractions were determined by ELISA.

(D) ApoE particle sizes were analyzed by dynamic light scattering (DLS).

(E) Representative images of astrocytic apoE particles (A-ApoE) and microglial apoE particles (M-ApoE) visualized with a transmission electron microscopy. Scale bar, 50 nm.

(F) Quantification of size of apoE particles/group. At least 50 apoE particles were used for the analysis. Data are presented as mean ± SEM. Statistical significance was determined with unpaired Student's t test. ***, $p < 0.001$.

RESULTS

Microglial apoE particles exhibited larger size than astrocytic apoE particles

To characterize the biological properties of apoE particles, we purified apoE particles from conditioned medium of primary microglia or astrocytes by immunoprecipitation (IP). Size-exclusion chromatography (SEC) analysis showed that microglial apoE particles were eluted from the column earlier than astrocytic apoE particles (Figures 1A–1C), suggesting that microglial apoE particles are on average larger than astrocytic apoE particles. Further, dynamic light scattering (DLS) (Figure 1D) and transmission electron microscopy (TEM) analyses showed that the average diameter of microglial apoE particles is around 30 nm, while that of astrocytic apoE particles is around 20 nm (Figures 1E and 1F). In addition, we also conducted the native gel electrophoresis with astrocytic and microglial apoE particles (Figure S1A). The results demonstrated that microglial apoE particles contain more large particles in comparison with astrocytic apoE particles (Figures S1A and S1B). Thus, the collective evidence from various analyses consistently indicates that microglial apoE particles are larger than astrocytic apoE particles.

Microglial apoE particle treatment altered neuron morphology and impaired synaptic functions

As a major lipid transporter, apoE has been reported to modulate maintenance of the neuronal functions in CNS.[36] Therefore, we compared the effect of microglial and astrocytic apoE particles on primary neurons. We observed that microglial apoE particles (6 μg/mL)[42] inhibited neurite growth, as indicated by alterations in neurite length and branch number (Figures 2A–2C). In addition, the total neuron number was reduced in microglial apoE particle treated group (Figures S2A and S2B), indicating the toxic effect of microglial apoE particles. Consistently, injection of microglial apoE particles into the hippocampus of wild-type (WT) mice led to a reduced neuronal density particularly in the local site of injection, when compared to the injection of astrocytic apoE particles (Figures S2C–S2E). Interestingly, we found that hippocampal injection of microglial apoE particles triggered marked gliosis (Figures S2C and S2F–S2I). Next we investigated the effect of glial apoE particles on synaptic function in primary neurons. Electrophysiological recordings showed that treatment of microglial apoE particles decreased frequencies of miniature excitatory postsynaptic current (mEPSC) in the treated neurons when compared with the treatment of astrocytic apoE particles (Figures 2D and 2E); while the amplitudes of mEPSC were similar between different treatments (Figure 2F). In addition, immunofluorescence staining showed that the expression of postsynaptic density protein 95 (PSD95) and synaptophysin (SYP) was lower in neurons treated with microglial apoE particles compared to that of neurons treated with astrocytic apoE particles (Figures 2G–2I).

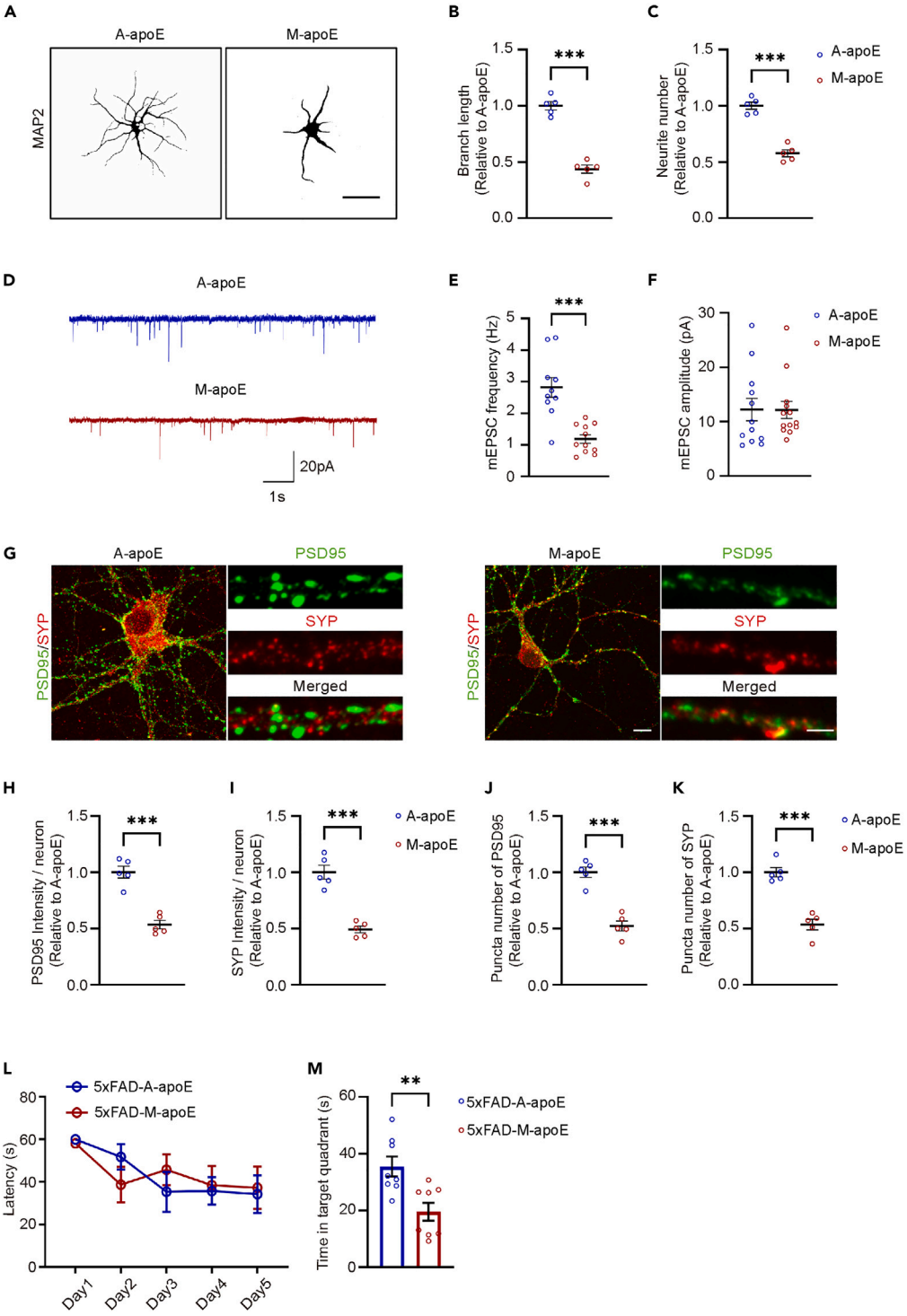

Figure 2. Microglial apoE particles are neurotoxic

(A) Sketched images of cultured neuron treated with astrocytic apoE particles and microglial apoE particles. Scale bar, 50 μm.

(B and C) Quantification of branch lengths and neurite numbers of cultured neurons ($n = 5$). The relative branch length and neurite number of neurons treated with microglial apoE particles were normalized to that of neurons treated with astrocytic apoE particles.

(D) Example of miniature EPSC traces recorded on cultured neurons treated with astrocytic apoE particles and microglial apoE particles. Scale bar, 1 s, 2 pA.

(E and F) Quantification of mEPSC frequency and amplitude. At least 10 neurons were recorded for the analysis.

Figure 2. *Continued*

(G) Representative confocal images of PSD-95 (green) and synaptophysin (red) of cultured neurons treated with astrocytic apoE particles and microglial apoE particles. Enlarged synapses are shown on the right. Scale bar, 10 μm.

(H–K) Quantification of PSD-95 and synaptophysin fluorescence intensity and puncta number per neuron (n = 5). Relative fluorescence intensity and puncta number from the microglial apoE particle treated group were normalized to that of the astrocytic apoE particles treated group.

(L) Performance of 5xFAD mice injected with astrocytic apoE particles (5xFAD-A-apoE) or microglial apoE particles (5xFAD-M-apoE) in the training phase of the MWM, n = 8 mice/group.

(M) Time that treated 5xFAD mice spent in target quadrant in the Probe test of MWM. Data are presented as mean ± SEM. Statistical significance was determined with unpaired Student's t test. For cellular experiments, n represents the number of independent experiments. **, $p < 0.01$, ***, $p < 0.001$.

Moreover, both of PSD95 and SYP puncta numbers were reduced upon microglial apoE particles treatment (Figures 2J and 2K). To evaluate the impact of apoE particles on neuronal function *in vivo*, we injected apoE particles (1 μg/μL) into the hippocampus of 5xFAD mice, a widely used transgenic AD mouse model.[43] In the Morris water maze (MWM) test, although 5xFAD mice injected with microglial apoE particles exhibited similar performance as the mice injected with astrocytic apoE particles in the training stage, these mice spent less time in the target quadrant during the probe test (Figures 2L and 2M), indicating that microglial apoE particles impaired spatial memory of 5xFAD mice. Together, these findings suggest that microglial apoE particles are more neurotoxic than astrocytic apoE particles.

Microglial apoE particles altered the transcriptomic profile of neurons and promoted neuronal senescence

To determine how microglial apoE particles affect neuronal function, we performed RNA sequencing (RNA-seq) analysis on primary neurons treated with vehicle or the two types of apoE particles. First, we carried out the principal component analysis (PCA) with three groups of samples and found that they were well separated, suggesting different treatments generated different effects (Figure S3A). Compared with the vehicle group, the expression of 585 genes was upregulated and the expression of 72 genes was downregulated upon treatment with astrocytic apoE particles, while 685 genes were upregulated and 156 genes were downregulated upon microglial apoE particles treatment (Figures S3B and S3C). Importantly, treatment with microglial apoE particles (M-apoE) upregulated 150 genes and downregulated 147 genes in neurons compared to the astrocytic apoE particle (A-apoE) treatment (Figure 3A). Kyoto Encyclopedia of Genes and Genomes (KEGG) enrichment analysis showed that these differentially expressed genes (DEGs) are enriched in pathways such as Epstein-Barr virus infection, cell cycle and cellular senescence (Figures 3B and S3D). Specifically, genes associated with aging and senescence such as H2-K1, H2-D1/Q6/Q4/Q7, H2-T22/23, GADD45a, and Igftbp3,[44] were upregulated in neurons treated with microglial apoE particles (Figure 3C). Meanwhile, genes associated with cellular mitosis and cell cycle[44,45] were downregulated after microglial apoE particles treatment, including Ccnb1, Ccna2, Ccnb2, Ccne2, Cdk1, and foxm1[45,46] (Figure 3C). Results from real-time (RT) PCR consistently validated differences in mRNA levels of these genes in neurons with different glial apoE particle treatments (Figures 3D and 3E). We next performed immunostaining to examine the expression of γH2AX and H3K27me3, two well-established markers for cellular senescence, in neurons treated with apoE particles derived from microglia or astrocytes (Figures 3F and 3H). As expected, both of γH2AX and H3K27me3 signals increased in neuronal nuclei after microglial apoE particle treatment, when compared to the astrocytic apoE particle treatment (Figures 3G–3I). These data suggest that microglial apoE particles promote neuronal senescence.

GPNMB mediated neuronal toxicity and senescence induced by microglial apoE particles

To investigate the underlying mechanisms of neurotoxicity caused by microglial apoE particles, we employed the mass spectrometry analysis to examine the protein composition of apoE particles derived from different cell types. Specifically, we identified a total of 315 proteins in microglial apoE particles and 677 proteins in astrocytic apoE particles (Figure S4A). Interestingly, 253 of these proteins were found in both types of glial apoE particles, while 62 proteins were exclusively detected in microglial apoE particles (Figure S4A). Notably, we observed that GPNMB identified in microglial apoE particles was the only protein overlapping with the protein module (Figure S4B) that has been associated with both AD pathogenesis and APOE genotype.[47] Further, we examined the level of GPNMB in glial apoE particles and found that microglial apoE particles had significantly higher levels of GPNMB compared to astrocytic apoE particles (Figure S4C). We next performed the delipidation experiment and detected GPNMB in the lipidated fractions "input" and "LRA pellet," but not in the lipid free fraction "PRA supernatant" (Figure S4D), suggesting that GPNMB is a component of lipidated apoE particles. We also analyzed AD related database (GSE44772) and found that the transcriptional level of *GPNMB*, a disease-associated microglia (DAM) marker gene, was significantly increased in the brain of AD patients (Figure S4E). Furthermore, the mRNA level of *GPNMB* was positively associated with Braak staging and brain atrophy in AD patients (Figures S4F and S4G).

To examine the role of GPNMB in microglial apoE particles, we purified microglial apoE particles from *Gpnmb*-KO mice (referred to as M-apoE-GPNMB). We treated neurons with differentially sourced apoE particles and observed that the absence of GPNMB mitigated the detrimental effects of microglial apoE particles on neuronal growth (M-apoE-GPNMB vs. M-apoE vs. vehicle) (Figures 4A–4C). Conversely, the addition of recombinant GPNMB protein (3 μg/mL) enabled astrocytic apoE particles (referred to as A-apoE + rGPNMB) to inhibit neuronal growth when compared with the vehicle or A-apoE treated groups (Figures 4A–4C). In addition, the levels of PSD95 and SYP in the neurons treated with M-apoE-GPNMB were comparable to that of the vehicle group, whereas neurons with A-apoE + rGPNMB treatment showed reduced PSD95 and SYP expression (Figures 4D–4F). We observed similar effects of M-apoE-GPNMB and A-apoE + rGPNMB on the frequencies of mEPSC (Figures 4G–4I); while the amplitudes of mESPC were not affected by these treatments. Further, the expression of γH2AX and H3K27me3 was increased in neurons treated with A-apoE + rGPNMB compared with vehicle or A-apoE groups, but both

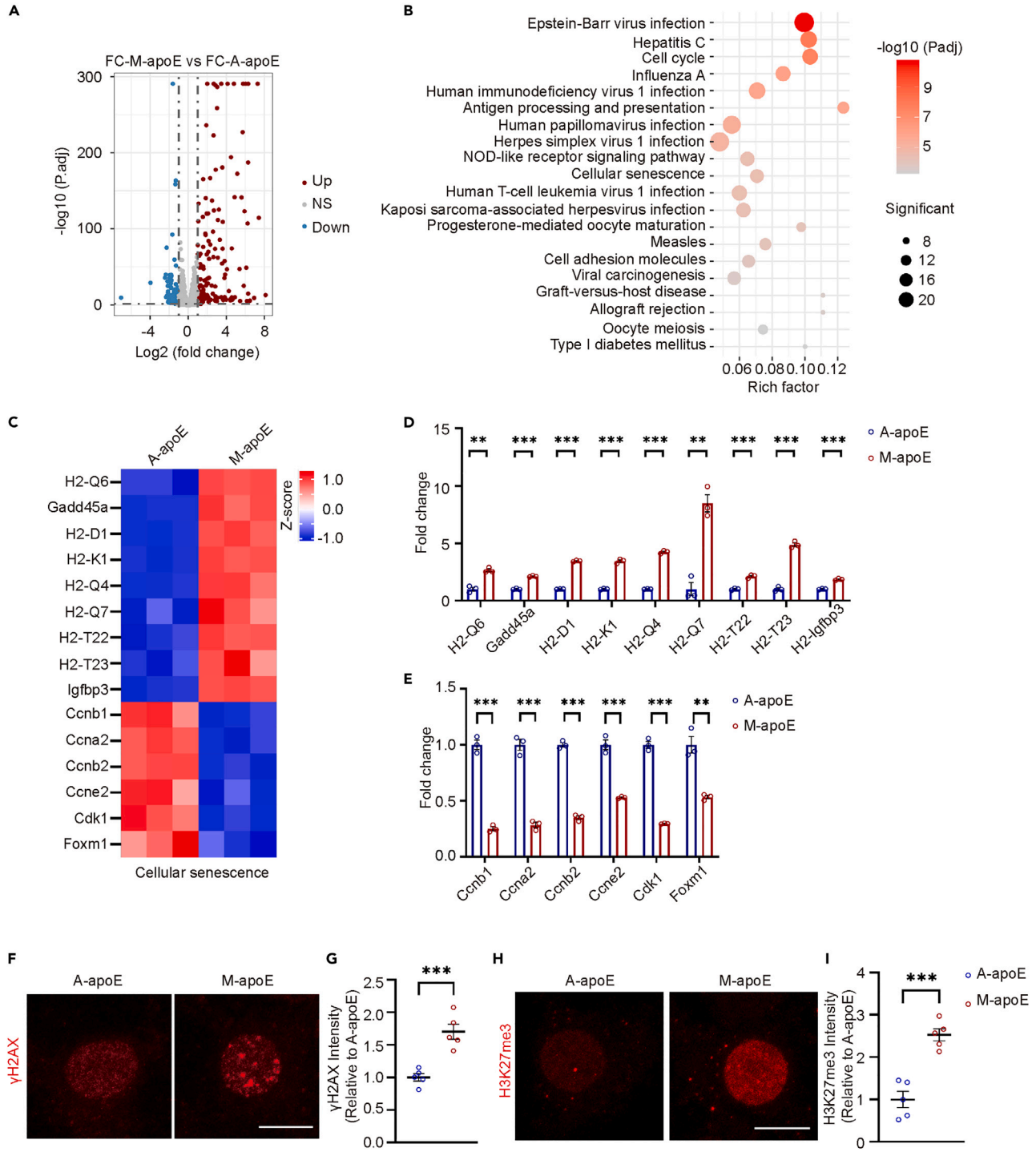

Figure 3. Microglial apoE particles promote neuronal senescence

(A) Volcano plot showing differentially expressed genes (DEGs) in cultured neurons treated with astrocytic apoE particles and microglial apoE particles, as measured by RNA-seq. The X axis specifies the log2 fold change (FC), and the Y axis represents the negative log10 of the *p.adj* values. Red and blue dots represent genes of which the expression levels are significantly increased or decreased in M-apoE versus A-apoE (filtering criteria: log2 FC > 0.5 and *p* value <0.05).

(B) Bubble chart showing the top 20 enriched KEGG pathway in M-apoE versus A-apoE. Dot sizes correspond to gene count number. Dots colored by *p* value. Rich factors indicate the percentage of significantly increased genes in whole pathway.

Figure 3. *Continued*

(C) Heatmap showing changes in gene expression of cellular senescence pathway. Z-scores normalization is used for the analysis. Red and blue squares represent genes whose expression level is significantly increased or decreased in M-apoE versus A-apoE (filtering criteria: log2 FC > 1 and p value <0.05).

(D and E) Real-time quantitative PCR (real-time qPCR) analysis of gene expression of cellular senescence pathways, normalized to a housekeeping gene (GAPDH). Data represent fold change relative to A-apoE and means ± SEM of three independent experiments.

(F and H) Representative confocal images of γH2AX (F) and H3K27me3 (H) staining of cultured neuron treated with astrocytic or microglial apoE particles. Scale bar, 10 μm.

(G and I) Quantification of γH2AX (G) and H3K27me3 (I) fluorescence intensity per cell (n = 5 independent experiments). Relative fluorescence intensity was normalized to neuron treated with astrocytic apoE particles. Data are presented as mean ± SEM. Statistical significance was determined with unpaired Student's t test. **, $p < 0.01$, ***, $p < 0.001$.

were reduced in neurons treated with M-apoE-GPNMB when compared with the M-apoE treatment (Figures 4J–4M). However, treatment with recombinant GPNMB (referred to as rGPNMB) in primary neuronal cultures had little effect on neuron numbers, branch lengths, and neurite numbers (Figures S5A–S5D). Together, these data indicate that GPNMB in microglial apoE particles plays a pivotal role in mediating neuronal toxicity and senescence induced by microglial apoE particles.

Microglial APOE4 led to more severe neurotoxicity

Next, we investigated whether apoE isoforms could impact the biochemical features and neurotoxicity of microglial apoE particles. We first evaluated the sizes of APOE3- and APOE4- particles secreted from microglia with target-replacement of human *APOE3* or *APOE4* (referred to as *APOE3*-TR or *APOE4*-TR) using non-denaturing gel electrophoresis followed by western blotting as described.[48] The apoE/lipoprotein particles were classified into three categories based on size: large particles (>690 kDa), medium particles (232–690 kDa), and small particles (<232 kDa). Compared to *APOE3*-TR primary microglia, *APOE4*-TR microglia secreted more large particles (12% more, ratio to total apoE/lipoprotein) and less small particles (~10% less, ratio to total apoE/lipoprotein) (Figures 5A and 5B). We then compared the effects of microglia-derived APOE3 and APOE4 particles on neuronal outgrowth using a co-culture system consisting of primary microglia and neurons (Figure 5C). Although *APOE3*-TR and *APOE*4-TR microglia similarly reduced neurite numbers compared to the control group in the co-culture system (Figures 5D and 5E), the *APOE4*-TR microglia-neuron co-culture exhibited a greater reduction in the neuronal lengths compared to the *APOE3*-TR microglia-neuron co-culture system (Figures 5D and 5F). These findings suggest that microglial apoE4 mediates a more severe neurotoxic effect, potentially amplifying the progression of AD.

DISCUSSION

ApoE plays multiple roles in brain health and impact the development of AD.[33,49] For instance, apoE assists in reducing cholesterol levels and to enhancing lipoprotein clearance.[49] Numerous studies have demonstrated that ApoE regulates various process associated with AD pathogenesis, including modulation of Aβ clearance, tau pathogenesis, lipid transport, and synaptic function.[30,32,50,51] While it is well established that apoE is primarily produced by astrocytes under physiological conditions, recent studies have revealed a marked increase in apoE expression in microglia during stress or disease conditions.[52] Nevertheless, the biological properties of microglia-derived apoE particles and the associated effects on neurons remain poorly understood. The data obtained from the current study demonstrate that apoE particles derived from primary microglia exhibit distinct sizes compared to those from primary astrocytes. Furthermore, microglia-derived apoE particles have detrimental effect on neurite growth and neuronal functions, ultimately contributing to neuronal senescence. Although numerous studies have highlighted a potential involvement of elevated microglial apoE level in the progression of neurodegenerative diseases such as AD, our study provide the first direct evidence supporting the contribution of microglia-derived apoE particles to neuronal senescence and toxicity.

In addition to amyloid and tau pathologies, a growing body of research suggests that neuroinflammation is a significant factor in the development of AD.[53–55] This notion is supported by genome-wide association studies (GWASs) analysis, which has identified associations between AD risk and genes related to inflammation, such as complement receptor-1 (*CR1*), *CD33*, and triggering receptor expressed on myeloid cells-2 (*TREM2*).[56–58] Targeting microglia and their associated pathways has emerged as a highly promising approach to mitigate the phenotypes associated with AD,[32,53,59,60] given that microglia are the primary cell type implicated in brain inflammation.[61] For instance, inhibition of IL-1 signaling has been shown to rescue cognitive impairment, attenuate tau pathology, and restore neuronal β-catenin pathway functionality in a mouse model of AD.[62] Previous investigations have demonstrated that heterozygous rare variants R47H, R62H and H157Y of TREM2 are associated with an increased risk of developing AD in African American, European and Asian populations.[56,63–66] Activation of TREM2 in AD mice improved microglial function and reduced amyloid deposition in the brain.[67–69] As a ligand for TREM2, ApoE may regulate microglial behaviors by modulating TREM2 pathway.[21,70,71] Additionally, it has been observed that inflammation influence the expression and secretion of apoE isoforms *in vitro*.[41] It is of great significance to investigate the potential differential regulation of microglial function by apoE particles derived from astrocytes and microglia, as well as the modulation of this process by apoE isoform. Furthermore, our study offers insights into the mechanism underlying microglia-neuron interaction and identifies a potential target within microglia for intervening neurotoxicity.

Mechanistically, we found that GPNMB mediates most of the detrimental effects induced by microglial apoE particles. Previous studies have identified GPNMB as a DAM gene that is upregulated in models of amyloidosis, tauopathy and aging.[72,73] Additionally, GPNMB has been linked to lipid homeostasis,[74] autophagy,[75] and immune response in AD.[53] As a single-pass transmembrane protein, it can be cleaved by a disintegrin and metalloproteinase 10 (ADAM10) or other extracellular proteases.[76] Elevated levels of soluble GPNMB in the

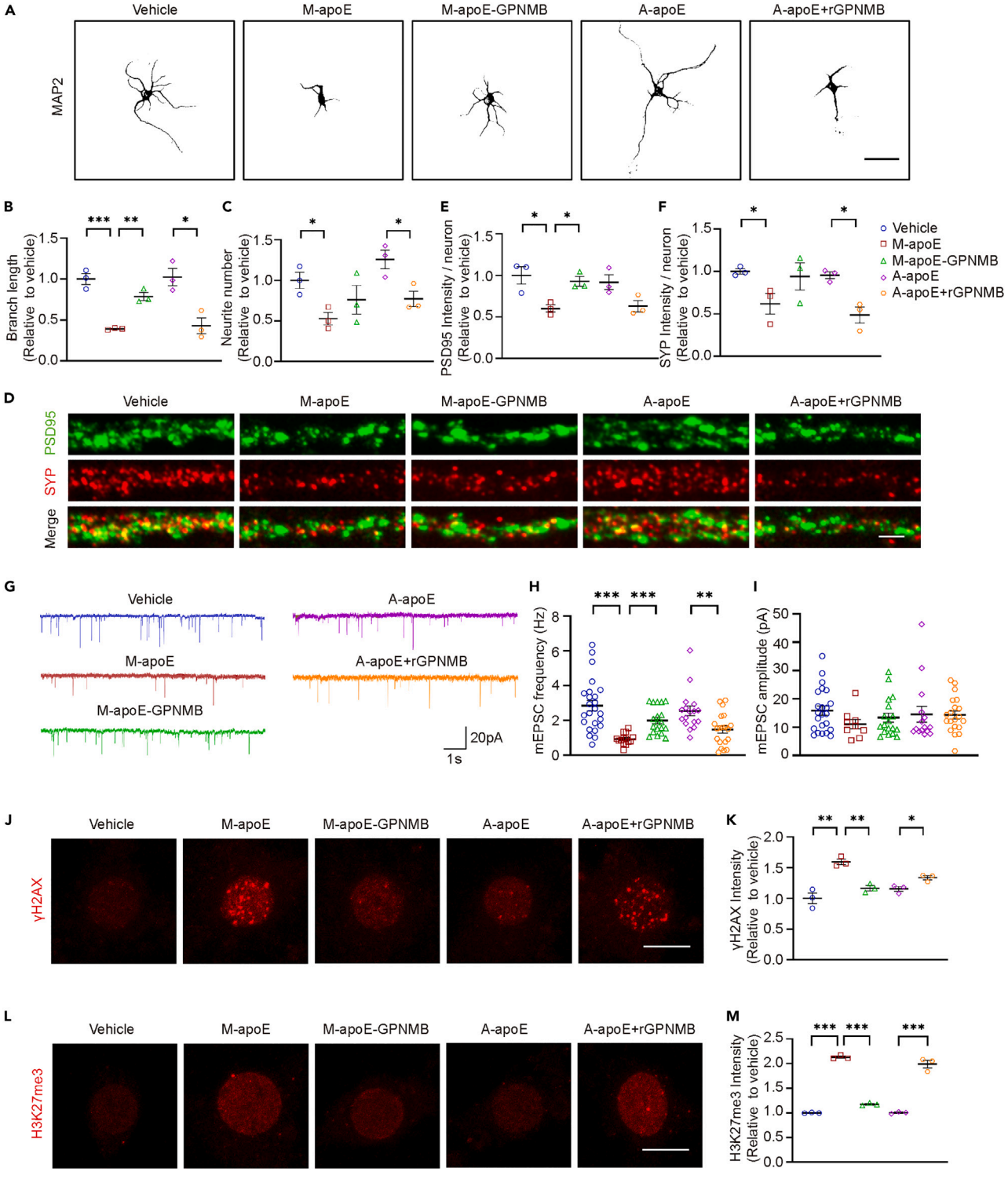

Figure 4. GPNMB plays a critical role in mediating neurotoxicity caused by microglial apoE particles

(A) Sketched images of cultured neurons (MAP2) treated with astrocytic apoE particles, microglial apoE particles, astrocytic apoE particles with recombinant GPNMB (rGPNMB) and GPNMB KO microglial apoE particles. Scale bar, 50 μm.

(B and C) Quantification of total length and branch number of cultured neuron (n = 3).

(D) Representative confocal images of PSD-95 (green) and synaptophysin (red) of cultured neuron treated as mentioned above. Scale bar, 10 μm.

Figure 4. *Continued*

(E and F) Quantification of PSD-95 and synaptophysin fluorescence intensity per neuron (n = 3). Relative fluorescence intensities from microglial apoE particle treated neurons were normalized to that of neurons treated with astrocytic apoE particles.

(G) Examples of miniature EPSC traces recorded on cultured neurons treated as mentioned above. Scale bar, 1 s, 2 pA.

(H and I) Quantification of mEPSC frequency and amplitude. At least 10 cultured neurons per group were used for the analysis.

(J and L) Representative confocal images of γH2AX (J) and H3K27me3 (L) of cultured neuron treated as mentioned above. Scale bar, 10 μm.

(K and M) Quantification of γH2AX (K) and H3K27me3 (M) fluorescence intensity per cell (n = 3). Relative fluorescence intensities were normalized to that of neurons treated with Vehicle. Data are presented as mean ± SEM. Statistical significance was determined with unpaired Student's t test. n represents the number of independent experiments. *, $p < 0.05$, **, $p < 0.01$, ***, $p < 0.001$.

cerebrospinal fluid (CSF) of AD patients have been reported,[77,78] and soluble GPNMB can interact with CD44 to affect astrocyte-mediated neuroinflammation.[79] Our analysis showed that GPNMB levels were elevated in AD patient brain samples and associated with disease severity. Furthermore, our findings suggest a potential role for GPNMB in regulating neuronal functions. Because lipoproteins can transport mRNAs in the circulation,[80] we do not exclude the potential contribution of the RNA content in apoE particles to the observed phenotypes. Further investigations are required to fully elucidate how microglial apoE complexes regulate AD pathogenesis.

It has been shown that mixed glial cells (~95% astrocytes) expressing the human APOE4 display a gain-of-toxic function and hinder neuronal growth.[81] Furthermore, astrocytic apoE alters neuronal cholesterol metabolism and memory through histone-acetylation, with *APOE4* displaying reduced ability to regulate metabolic and epigenetic process in neurons compared to *APOE3*.[42] However, the impact of different APOE isoforms expressed by microglia on neurite outgrowth remains unclear. In the current study, we observed neurotoxicity associated with *APOE4*-TR microglia compared to *APOE3*-TR microglia, which aligns with a recent publication that demonstrates the

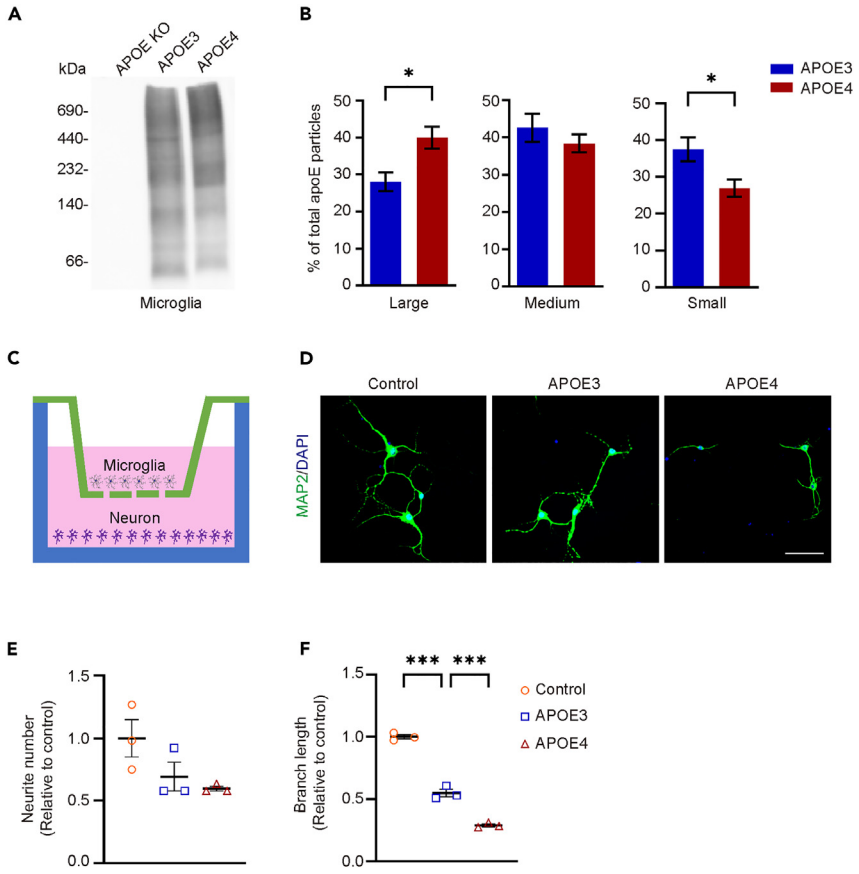

Figure 5. Microglial APOE4 particles exhibit distinct biochemical features and severer neurotoxicity compared with microglial APOE3 particles

(A and B) ApoE particles from conditioned medium of primary *APOE3*-TR or *APOE4*-TR microglia were analyzed by native gel electrophoresis. Particle sizes were defined as large (>690 kDa), medium (232 kDa–720 kDa), and small (<232 kDa). The percentages of apoE particles in different size categories were quantified.

(C) Schematic diagram of microglia-neuron co-culture system.

(D) Neurons co-cultured with *APOE3*-TR or *APOE4*-TR microglia were stained for MAP2. Neuronal culture without microglia in the top insert was used as the control group. Scale bar, 20 μm.

(E and F) Neurite lengths (from initiation site) and numbers were quantified and normalized to that of the control. Data are presented as mean ± SEM (n = 3–5). n represents the number of independent experiments. Statistical significance was determined with t test or one-way ANOVA. *, $p < 0.05$; ***, $p < 0.001$.

exacerbation of neuronal senescence in *APOE4*-TR mice.[82] This phenotype may be attributed, at least in part, to the larger size of microglial APOE4 particles, because previous studies have linked larger-sized apoE particles with neurotoxicity.[36,83] Additionally, we observed lower GPNMB/APOE ratio in APOE4 particles, compared to that in APOE3 particles, suggesting that GPNMB might not be the primary culprit for the neurotoxic effects of microglial APOE4 (data not shown). Previous studies have identified numerous factors contribute to the toxic effect of APOE4, including elevated pro-inflammatory responses, dysregulated lipid metabolism, self-aggregation, and reduced affinity for binding to receptors.[84,85] Moreover, other differing components between microglial APOE4 and APOE3 particles may also influence the varying degrees of neurotoxicity exhibited by these particles, emphasizing the necessity for further investigations in future studies.

In summary, our results demonstrate critical roles of apoE particles and APOE isoforms in regulating neuronal morphology and function. These findings should be further verified in additional animal models. A deeper comprehension of the molecular mechanisms and intracellular pathways involved in apoE-mediated microglial functions may provide insight into how APOE isoforms contribute to AD pathogenesis.

Limitations of the study

Firstly, our studies are mainly performed *in vitro*. Therefore, the physiological relevance of our findings and the potential toxicity related to the large-sized particles derived from microglia need to be further explored *in vivo*. Secondly, aggregation and lipidation may contribute to the increased size of microglial apoE particles. Hence, further research is warranted to investigate the specific components of these particles and their functional significance. Thirdly, there are discrepancies in particle size between our data and previous reports; we speculate that these differences may be attributed to variation in materials, resources and experimental procedures. Lastly, because microglia typically express lower level of apoE under physiology conditions, the high concentration of apoE particles used in our study might enhance the approach.

STAR★METHODS

Detailed methods are provided in the online version of this paper and include the following:

- KEY RESOURCES TABLE
- RESOURCE AVAILABILITY
  - Lead contact
  - Materials availability
  - Data and code availability
- EXPERIMENTAL MODEL AND SUBJECT DETAILS
  - Mice
  - Primary cell culture
  - Study approval
- METHOD DETAILS
  - ApoE/lipoprotein particles purification
  - ApoE ELISA
  - Fast protein liquid chromatography
  - Dynamic light scattering
  - Electron microscopy and immunoelectron microscopy
  - Immunofluorescence staining
  - Immunohistochemistry staining
  - RNA extraction and quantitative RT-PCR
  - Western Blot
  - Delipidation
  - Electrophysiological recording
  - RNA sequencing analysis
  - ApoE particle injection
  - Morris Water Maze
  - Mass spectrometry
  - Analysis of apolipoprotein E gene particle sizes by native PAGE
- QUANTIFICATION AND STATISTICAL ANALYSIS

SUPPLEMENTAL INFORMATION

Supplemental information can be found online at https://doi.org/10.1016/j.isci.2024.110006.

ACKNOWLEDGMENTS

We thank the National Key R&D Program of China 2021ZD0202402 (H.X.), the National Key R&D Program of China 2021YFA1101401 (Y.Z.), the National Natural Science Foundation of China grants 82071213 (Y.Z.), 82271472 (H. Zhang), 92049202, and 92149303 (H.X.), a start-up

funding from Xiamen University (Y.Z.), the Lingang Laboratory (grant no. LG-GG-202401-ADAD060200), the Science and Technology Research Program of Chongqing Municipal Education Commission (KJQN202200479), the Natural Science Foundation of Chongqing (CSTB2022NSCQ-LZX0033), and CQMU Program for Youth Innovation in Future Medicine (W0158). We thank Qiang Liu from University of Science and Technology of China; Zhihan Wang at West China School of Basic Medical Sciences & Forensic Medicine at Sichuan University; and Luming Yao, Caiming Wu, Baoying Xie, Haiping Zheng, Jingru Huang, Qingfeng Liu, Xiang You, Zhenni Xu, Yaying Wu and Hao Sun at Core Facility of Biomedical Sciences at Xiamen University for providing technical support.

AUTHOR CONTRIBUTIONS

H.X., Y.Z., H. Zhang, and Z.W. designed the research; N.W., L.C., X.P., Z.L., L.H., M.W., L.S., T.G., and F.H. performed experimental work; H.L., H. Zheng., X.-f.C., L.L., Y.-w.Z., X.W., J.Z., and K.G. analyzed and contributed reagents/materials/analysis tools; N.W., L.C., Z.W., H. Zhang, and Y.Z. wrote the manuscript. All authors have read and approved the article.

DECLARATION OF INTERESTS

The authors declare no competing interests.

Received: August 24, 2023
Revised: December 13, 2023
Accepted: May 14, 2024
Published: May 16, 2024

REFERENCES

1. (2023). 2023 Alzheimer's disease facts and figures. Alzheimer's Dementia *19*, 1598–1695. https://doi.org/10.1002/alz.13016.
2. Bu, G. (2009). Apolipoprotein E and its receptors in Alzheimer's disease: pathways, pathogenesis and therapy. Nat. Rev. Neurosci. *10*, 333–344. https://doi.org/10.1038/nrn2620.
3. Blennow, K., de Leon, M.J., and Zetterberg, H. (2006). Alzheimer's disease. Lancet *368*, 387–403. https://doi.org/10.1016/S0140-6736(06)69113-7.
4. DeTure, M.A., and Dickson, D.W. (2019). The neuropathological diagnosis of Alzheimer's disease. Mol. Neurodegener. *14*, 32. https://doi.org/10.1186/s13024-019-0333-5.
5. Mandrekar-Colucci, S., and Landreth, G.E. (2010). Microglia and inflammation in Alzheimer's disease. CNS Neurol. Disord. Drug Targets *9*, 156–167.
6. Egensperger, R., Kösel, S., von Eitzen, U., and Graeber, M.B. (1998). Microglial activation in Alzheimer disease: Association with APOE genotype. Brain Pathol. *8*, 439–447.
7. Bolos, M., Perea, J.R., and Avila, J. (2017). Alzheimer's disease as an inflammatory disease. Biomol. Concepts *8*, 37–43. https://doi.org/10.1515/bmc-2016-0029.
8. Wes, P.D., Sayed, F.A., Bard, F., and Gan, L. (2016). Targeting microglia for the treatment of Alzheimer's Disease. Glia *64*, 1710–1732. https://doi.org/10.1002/glia.22988.
9. Wang, X., Allen, M., Li, S., Quicksall, Z.S., Patel, T.A., Carnwath, T.P., Reddy, J.S., Carrasquillo, M.M., Lincoln, S.J., Nguyen, T.T., et al. (2020). Deciphering cellular transcriptional alterations in Alzheimer's disease brains. Mol. Neurodegener. *15*, 38. https://doi.org/10.1186/s13024-020-00392-6.
10. Guo, T., Zhang, D., Zeng, Y., Huang, T.Y., Xu, H., and Zhao, Y. (2020). Molecular and cellular mechanisms underlying the pathogenesis of Alzheimer's disease. Mol. Neurodegener. *15*, 40. https://doi.org/10.1186/s13024-020-00391-7.
11. Chen, Y., and Colonna, M. (2022). Two-faced behavior of microglia in Alzheimer's disease. Nat. Neurosci. *25*, 3–4. https://doi.org/10.1038/s41593-021-00963-w.
12. Kosoy, R., Fullard, J.F., Zeng, B., Bendl, J., Dong, P., Rahman, S., Kleopoulos, S.P., Shao, Z., Girdhar, K., Humphrey, J., et al. (2022). Genetics of the human microglia regulome refines Alzheimer's disease risk loci. Nat. Genet. *54*, 1145–1154. https://doi.org/10.1038/s41588-022-01149-1.
13. Dejanovic, B., Wu, T., Tsai, M.-C., Graykowski, D., Gandham, V.D., Rose, C.M., Bakalarski, C.E., Ngu, H., Wang, Y., Pandey, S., et al. (2022). Complement C1q-dependent excitatory and inhibitory synapse elimination by astrocytes and microglia in Alzheimer's disease mouse models. Nat. Aging *2*, 837–850. https://doi.org/10.1038/s43587-022-00281-1.
14. Ransohoff, R.M., and Perry, V.H. (2009). Microglial physiology: unique stimuli, specialized responses. Annu. Rev. Immunol. *27*, 119–145. https://doi.org/10.1146/annurev.immunol.021908.132528.
15. Terzioglu, G., and Young-Pearse, T.L. (2023). Microglial function, INPP5D/SHIP1 signaling, and NLRP3 inflammasome activation: implications for Alzheimer's disease. Mol. Neurodegener. *18*, 89. https://doi.org/10.1186/s13024-023-00674-9.
16. Jeong, H.K., Ji, K., Min, K., and Joe, E.H. (2013). Brain inflammation and microglia: facts and misconceptions. Exp. Neurobiol. *22*, 59–67. https://doi.org/10.5607/en.2013.22.2.59.
17. Akiyoshi, R., Wake, H., Kato, D., Horiuchi, H., Ono, R., Ikegami, A., Haruwaka, K., Omori, T., Tachibana, Y., Moorhouse, A.J., and Nabekura, J. (2018). Microglia Enhance Synapse Activity to Promote Local Network Synchronization. eNeuro *5*, ENEURO.0088-18.2018. https://doi.org/10.1523/ENEURO.0088-18.2018.
18. Parkhurst, C.N., Yang, G., Ninan, I., Savas, J.N., Yates, J.R., 3rd, Lafaille, J.J., Hempstead, B.L., Littman, D.R., and Gan, W.B. (2013). Microglia promote learning-dependent synapse formation through brain-derived neurotrophic factor. Cell *155*, 1596–1609. https://doi.org/10.1016/j.cell.2013.11.030.
19. Xu, Z.X., Kim, G.H., Tan, J.W., Riso, A.E., Sun, Y., Xu, E.Y., Liao, G.Y., Xu, H., Lee, S.H., Do, N.Y., et al. (2020). Elevated protein synthesis in microglia causes autism-like synaptic and behavioral aberrations. Nat. Commun. *11*, 1797. https://doi.org/10.1038/s41467-020-15530-3.
20. Tzioras, M., McGeachan, R.I., Durrant, C.S., and Spires-Jones, T.L. (2023). Synaptic degeneration in Alzheimer disease. Nat. Rev. Neurol. *19*, 19–38. https://doi.org/10.1038/s41582-022-00749-z.
21. Wang, N., Wang, M., Jeevaratnam, S., Rosenberg, C., Ikezu, T.C., Shue, F., Doss, S.V., Alnobani, A., Martens, Y.A., Wren, M., et al. (2022). Opposing effects of apoE2 and apoE4 on microglial activation and lipid metabolism in response to demyelination. Mol. Neurodegener. *17*, 75. https://doi.org/10.1186/s13024-022-00577-1.
22. Ransohoff, R.M., and El Khoury, J. (2015). Microglia in Health and Disease. Cold Spring Harbor Perspect. Biol. *8*, a020560. https://doi.org/10.1101/cshperspect.a020560.
23. Southam, K.A., Vincent, A.J., and Small, D.H. (2016). Do Microglia Default on Network Maintenance in Alzheimer's Disease? J. Alzheimers Dis. *51*, 657–669. https://doi.org/10.3233/JAD-151075.
24. Efthymiou, A.G., and Goate, A.M. (2017). Late onset Alzheimer's disease genetics implicates microglial pathways in disease risk. Mol. Neurodegener. *12*, 43. https://doi.org/10.1186/s13024-017-0184-x.
25. Shi, Y., and Holtzman, D.M. (2018). Interplay between innate immunity and Alzheimer disease: APOE and TREM2 in the spotlight. Nat. Rev. Immunol. *18*, 759–772. https://doi.org/10.1038/s41577-018-0051-1.
26. Bido, S., Muggeo, S., Massimino, L., Marzi, M.J., Giannelli, S.G., Melacini, E., Nannoni, M., Gambarè, D., Bellini, E., Ordazzo, G., et al. (2021). Author Correction: Microglia-specific overexpression of alpha-synuclein

leads to severe dopaminergic neurodegeneration by phagocytic exhaustion and oxidative toxicity. Nat. Commun. *12*, 7359. https://doi.org/10.1038/s41467-021-27737-z.

27. Leng, F., and Edison, P. (2021). Neuroinflammation and microglial activation in Alzheimer disease: where do we go from here? Nat. Rev. Neurol. *17*, 157–172. https://doi.org/10.1038/s41582-020-00435-y.
28. Ghebranious, N., Ivacic, L., Mallum, J., and Dokken, C. (2005). Detection of ApoE E2, E3 and E4 alleles using MALDI-TOF mass spectrometry and the homogeneous mass-extend technology. Nucleic Acids Res. *33*, e149. https://doi.org/10.1093/nar/gni155.
29. Mahley, R.W. (1988). Apolipoprotein E: cholesterol transport protein with expanding role in cell biology. Science *240*, 622–630. https://doi.org/10.1126/science.3283935.
30. Liu, C.C., Liu, C.C., Kanekiyo, T., Xu, H., and Bu, G. (2013). Apolipoprotein E and Alzheimer disease: risk, mechanisms and therapy. Nat. Rev. Neurol. *9*, 106–118. https://doi.org/10.1038/nrneurol.2012.263.
31. Najm, R., Jones, E.A., and Huang, Y. (2019). Apolipoprotein E4, inhibitory network dysfunction, and Alzheimer's disease. Mol. Neurodegener. *14*, 24. https://doi.org/10.1186/s13024-019-0324-6.
32. Yamazaki, Y., Zhao, N., Caulfield, T.R., Liu, C.C., and Bu, G. (2019). Apolipoprotein E and Alzheimer disease: pathobiology and targeting strategies. Nat. Rev. Neurol. *15*, 501–518. https://doi.org/10.1038/s41582-019-0228-7.
33. Fernandez-Calle, R., Konings, S.C., Frontinan-Rubio, J., Garcia-Revilla, J., Camprubi-Ferrer, L., Svensson, M., Martinson, I., Boza-Serrano, A., Venero, J.L., Nielsen, H.M., et al. (2022). APOE in the bullseye of neurodegenerative diseases: impact of the APOE genotype in Alzheimer's disease pathology and brain diseases. Mol. Neurodegener. *17*, 62. https://doi.org/10.1186/s13024-022-00566-4.
34. Ulrich, J.D., Ulland, T.K., Mahan, T.E., Nyström, S., Nilsson, K.P., Song, W.M., Zhou, Y., Reinartz, M., Choi, S., Jiang, H., et al. (2018). ApoE facilitates the microglial response to amyloid plaque pathology. J. Exp. Med. *215*, 1047–1058. https://doi.org/10.1084/jem.20171265.
35. Huang, Y., and Mahley, R.W. (2014). Apolipoprotein E: structure and function in lipid metabolism, neurobiology, and Alzheimer's diseases. Neurobiol. Dis. *72*, 3–12. https://doi.org/10.1016/j.nbd.2014.08.025.
36. Husain, M.A., Laurent, B., and Plourde, M. (2021). APOE and Alzheimer's Disease: From Lipid Transport to Physiopathology and Therapeutics. Front. Neurosci. *15*, 630502. https://doi.org/10.3389/fnins.2021.630502.
37. Fu, Y., Zhao, J., Atagi, Y., Nielsen, H.M., Liu, C.C., Zheng, H., Shinohara, M., Kanekiyo, T., and Bu, G. (2016). Apolipoprotein E lipoprotein particles inhibit amyloid-beta uptake through cell surface heparan sulphate proteoglycan. Mol. Neurodegener. *11*, 37. https://doi.org/10.1186/s13024-016-0099-y.
38. Deczkowska, A., Keren-Shaul, H., Weiner, A., Colonna, M., Schwartz, M., and Amit, I. (2018). Disease-Associated Microglia: A Universal Immune Sensor of Neurodegeneration. Cell *173*, 1073–1081. https://doi.org/10.1016/j.cell.2018.05.003.
39. Shi, Y., Manis, M., Long, J., Wang, K., Sullivan, P.M., Remolina Serrano, J., Hoyle, R., and Holtzman, D.M. (2019). Microglia drive APOE-dependent neurodegeneration in a tauopathy mouse model. J. Exp. Med. *216*, 2546–2561. https://doi.org/10.1084/jem.20190980.
40. Rangaraju, S., Dammer, E.B., Raza, S.A., Gao, T., Xiao, H., Betarbet, R., Duong, D.M., Webster, J.A., Hales, C.M., Lah, J.J., et al. (2018). Quantitative proteomics of acutely-isolated mouse microglia identifies novel immune Alzheimer's disease-related proteins. Mol. Neurodegener. *13*, 34. https://doi.org/10.1186/s13024-018-0266-4.
41. Lanfranco, M.F., Sepulveda, J., Kopetsky, G., and Rebeck, G.W. (2021). Expression and secretion of apoE isoforms in astrocytes and microglia during inflammation. Glia *69*, 1478–1493. https://doi.org/10.1002/glia.23974.
42. Li, X., Zhang, J., Li, D., He, C., He, K., Xue, T., Wan, L., Zhang, C., and Liu, Q. (2021). Astrocytic ApoE reprograms neuronal cholesterol metabolism and histone-acetylation-mediated memory. Neuron *109*, 957–970.e8. https://doi.org/10.1016/j.neuron.2021.01.005.
43. Oakley, H., Cole, S.L., Logan, S., Maus, E., Shao, P., Craft, J., Guillozet-Bongaarts, A., Ohno, M., Disterhoft, J., Van Eldik, L., et al. (2006). Intraneuronal beta-amyloid aggregates, neurodegeneration, and neuron loss in transgenic mice with five familial Alzheimer's disease mutations: potential factors in amyloid plaque formation. J. Neurosci. *26*, 10129–10140. https://doi.org/10.1523/JNEUROSCI.1202-06.2006.
44. Kellogg, C.M., Pham, K., Machalinski, A.H., Porter, H.L., Blankenship, H.E., Tooley, K., Stout, M.B., Rice, H.C., Sharpe, A.L., Beckstead, M.J., et al. (2023). Microglial MHC-I induction with aging and Alzheimer's is conserved in mouse models and humans. Preprint at bioRxiv. https://doi.org/10.1101/2023.03.07.531435.
45. Liao, G.B., Li, X.Z., Zeng, S., Liu, C., Yang, S.M., Yang, L., Hu, C.J., and Bai, J.Y. (2018). Regulation of the master regulator FOXM1 in cancer. Cell Commun. Signal. *16*, 57. https://doi.org/10.1186/s12964-018-0266-6.
46. Malumbres, M. (2014). Cyclin-dependent kinases. Genome Biol. *15*, 122. https://doi.org/10.1186/gb4184.
47. Johnson, E.C.B., Carter, E.K., Dammer, E.B., Duong, D.M., Gerasimov, E.S., Liu, Y., Liu, J., Betarbet, R., Ping, L., Yin, L., et al. (2022). Large-scale deep multi-layer analysis of Alzheimer's disease brain reveals strong proteomic disease-related changes not observed at the RNA level. Nat. Neurosci. *25*, 213–225. https://doi.org/10.1038/s41593-021-00999-y.
48. Hu, J., Liu, C.C., Chen, X.F., Zhang, Y.W., Xu, H., and Bu, G. (2015). Opposing effects of viral mediated brain expression of apolipoprotein E2 (apoE2) and apoE4 on apoE lipidation and Abeta metabolism in apoE4-targeted replacement mice. Mol. Neurodegener. *10*, 6. https://doi.org/10.1186/s13024-015-0001-3.
49. Kloske, C.M., and Wilcock, D.M. (2020). The Important Interface Between Apolipoprotein E and Neuroinflammation in Alzheimer's Disease. Front. Immunol. *11*, 754. https://doi.org/10.3389/fimmu.2020.00754.
50. Kim, J., Basak, J.M., and Holtzman, D.M. (2009). The role of apolipoprotein E in Alzheimer's disease. Neuron *63*, 287–303. https://doi.org/10.1016/j.neuron.2009.06.026.
51. Shi, Y., Yamada, K., Liddelow, S.A., Smith, S.T., Zhao, L., Luo, W., Tsai, R.M., Spina, S., Grinberg, L.T., Rojas, J.C., et al. (2017). ApoE4 markedly exacerbates tau-mediated neurodegeneration in a mouse model of tauopathy. Nature *549*, 523–527. https://doi.org/10.1038/nature24016.
52. de Chaves, E.P., and Narayanaswami, V. (2008). Apolipoprotein E and cholesterol in aging and disease in the brain. Future Lipidol. *3*, 505–530. https://doi.org/10.2217/17460875.3.5.505.
53. Huttenrauch, M., Ogorek, I., Klafki, H., Otto, M., Stadelmann, C., Weggen, S., Wiltfang, J., and Wirths, O. (2018). Glycoprotein NMB: a novel Alzheimer's disease associated marker expressed in a subset of activated microglia. Acta Neuropathol. Commun. *6*, 108. https://doi.org/10.1186/s40478-018-0612-3.
54. Walker, K.A., Le Page, L.M., Terrando, N., Duggan, M.R., Heneka, M.T., and Bettcher, B.M. (2023). The role of peripheral inflammatory insults in Alzheimer's disease: a review and research roadmap. Mol. Neurodegener. *18*, 37. https://doi.org/10.1186/s13024-023-00627-2.
55. Wareham, L.K., Liddelow, S.A., Temple, S., Benowitz, L.I., Di Polo, A., Wellington, C., Goldberg, J.L., He, Z., Duan, X., Bu, G., et al. (2022). Solving neurodegeneration: common mechanisms and strategies for new treatments. Mol. Neurodegener. *17*, 23. https://doi.org/10.1186/s13024-022-00524-0.
56. Guerreiro, R., Wojtas, A., Bras, J., Carrasquillo, M., Rogaeva, E., Majounie, E., Cruchaga, C., Sassi, C., Kauwe, J.S.K., Younkin, S., et al. (2013). TREM2 variants in Alzheimer's disease. N. Engl. J. Med. *368*, 117–127. https://doi.org/10.1056/NEJMoa1211851.
57. Hollingworth, P., Harold, D., Sims, R., Gerrish, A., Lambert, J.C., Carrasquillo, M.M., Abraham, R., Hamshere, M.L., Pahwa, J.S., Moskvina, V., et al. (2011). Common variants at ABCA7, MS4A6A/MS4A4E, EPHA1, CD33 and CD2AP are associated with Alzheimer's disease. Nat. Genet. *43*, 429–435. https://doi.org/10.1038/ng.803.
58. Lambert, J.C., Heath, S., Even, G., Campion, D., Sleegers, K., Hiltunen, M., Combarros, O., Zelenika, D., Bullido, M.J., Tavernier, B., et al. (2009). Genome-wide association study identifies variants at CLU and CR1 associated with Alzheimer's disease. Nat. Genet. *41*, 1094–1099. https://doi.org/10.1038/ng.439.
59. Williams, T., Borchelt, D.R., and Chakrabarty, P. (2020). Therapeutic approaches targeting Apolipoprotein E function in Alzheimer's disease. Mol. Neurodegener. *15*, 8. https://doi.org/10.1186/s13024-020-0358-9.
60. Huang, Y., Liu, B., Sinha, S.C., Amin, S., and Gan, L. (2023). Mechanism and therapeutic potential of targeting cGAS-STING signaling in neurological disorders. Mol. Neurodegener. *18*, 79. https://doi.org/10.1186/s13024-023-00672-x.
61. Baxter, P.S., Dando, O., Emelianova, K., He, X., McKay, S., Hardingham, G.E., and Qiu, J. (2021). Microglial identity and inflammatory responses are controlled by the combined effects of neurons and astrocytes. Cell Rep. *34*, 108882. https://doi.org/10.1016/j.celrep.2021.108882.
62. Kitazawa, M., Cheng, D., Tsukamoto, M.R., Koike, M.A., Wes, P.D., Vasilevko, V., Cribbs, D.H., and LaFerla, F.M. (2011). Blocking IL-1 signaling rescues cognition, attenuates tau pathology, and restores neuronal beta-catenin pathway function in an Alzheimer's disease model. J. Immunol. *187*, 6539–6549. https://doi.org/10.4049/jimmunol.1100620.

63. Jin, S.C., Benitez, B.A., Karch, C.M., Cooper, B., Skorupa, T., Carrell, D., Norton, J.B., Hsu, S., Harari, O., Cai, Y., et al. (2014). Coding variants in TREM2 increase risk for Alzheimer's disease. Hum. Mol. Genet. *23*, 5838–5846. https://doi.org/10.1093/hmg/ddu277.
64. Jiang, T., Tan, L., Chen, Q., Tan, M.S., Zhou, J.S., Zhu, X.C., Lu, H., Wang, H.F., Zhang, Y.D., and Yu, J.T. (2016). A rare coding variant in TREM2 increases risk for Alzheimer's disease in Han Chinese. Neurobiol. Aging *42*, 217.e1–217.e3. https://doi.org/10.1016/j.neurobiolaging.2016.02.023.
65. Jonsson, T., Stefansson, H., Steinberg, S., Jonsdottir, I., Jonsson, P.V., Snaedal, J., Bjornsson, S., Huttenlocher, J., Levey, A.I., Lah, J.J., et al. (2013). Variant of TREM2 associated with the risk of Alzheimer's disease. N. Engl. J. Med. *368*, 107–116. https://doi.org/10.1056/NEJMoa1211103.
66. Jain, N., and Ulrich, J.D. (2022). TREM2 and microglia exosomes: a potential highway for pathological tau. Mol. Neurodegener. *17*, 73. https://doi.org/10.1186/s13024-022-00581-5.
67. van Lengerich, B., Zhan, L., Xia, D., Chan, D., Joy, D., Park, J.I., Tatarakis, D., Calvert, M., Hummel, S., Lianoglou, S., et al. (2023). A TREM2-activating antibody with a blood-brain barrier transport vehicle enhances microglial metabolism in Alzheimer's disease models. Nat. Neurosci. *26*, 416–429. https://doi.org/10.1038/s41593-022-01240-0.
68. Price, B.R., Sudduth, T.L., Weekman, E.M., Johnson, S., Hawthorne, D., Woolums, A., and Wilcock, D.M. (2020). Therapeutic Trem2 activation ameliorates amyloid-beta deposition and improves cognition in the 5XFAD model of amyloid deposition. J. Neuroinflammation *17*, 238. https://doi.org/10.1186/s12974-020-01915-0.
69. Hou, J., Chen, Y., Grajales-Reyes, G., and Colonna, M. (2022). TREM2 dependent and independent functions of microglia in Alzheimer's disease. Mol. Neurodegener. *17*, 84. https://doi.org/10.1186/s13024-022-00588-y.
70. Atagi, Y., Liu, C.C., Painter, M.M., Chen, X.F., Verbeeck, C., Zheng, H., Li, X., Rademakers, R., Kang, S.S., Xu, H., et al. (2015). Apolipoprotein E Is a Ligand for Triggering Receptor Expressed on Myeloid Cells 2 (TREM2). J. Biol. Chem. *290*, 26043–26050. https://doi.org/10.1074/jbc.M115.679043.
71. Li, R.Y., Qin, Q., Yang, H.C., Wang, Y.Y., Mi, Y.X., Yin, Y.S., Wang, M., Yu, C.J., and Tang, Y. (2022). TREM2 in the pathogenesis of AD: a lipid metabolism regulator and potential metabolic therapeutic target. Mol. Neurodegener. *17*, 40. https://doi.org/10.1186/s13024-022-00542-y.
72. Kang, S.S., Ebbert, M.T.W., Baker, K.E., Cook, C., Wang, X., Sens, J.P., Kocher, J.P., Petrucelli, L., and Fryer, J.D. (2018). Microglial translational profiling reveals a convergent APOE pathway from aging, amyloid, and tau. J. Exp. Med. *215*, 2235–2245. https://doi.org/10.1084/jem.20180653.
73. Kim, D.W., Tu, K.J., Wei, A., Lau, A.J., Gonzalez-Gil, A., Cao, T., Braunstein, K., Ling, J.P., Troncoso, J.C., Wong, P.C., et al. (2022). Amyloid-beta and tau pathologies act synergistically to induce novel disease stage-specific microglia subtypes. Mol. Neurodegener. *17*, 83. https://doi.org/10.1186/s13024-022-00589-x.
74. Smith, A.M., Davey, K., Tsartsalis, S., Khozoie, C., Fancy, N., Tang, S.S., Liaptsi, E., Weinert, M., McGarry, A., Muirhead, R.C.J., et al. (2022). Diverse human astrocyte and microglial transcriptional responses to Alzheimer's pathology. Acta Neuropathol. *143*, 75–91. https://doi.org/10.1007/s00401-021-02372-6.
75. Zhu, Z., Liu, Y., Li, X., Zhang, L., Liu, H., Cui, Y., Wang, Y., and Zhao, D. (2022). GPNMB mitigates Alzheimer's disease and enhances autophagy via suppressing the mTOR signal. Neurosci. Lett. *767*, 136300. https://doi.org/10.1016/j.neulet.2021.136300.
76. Rose, A.A.N., Annis, M.G., Dong, Z., Pepin, F., Hallett, M., Park, M., and Siegel, P.M. (2010). ADAM10 releases a soluble form of the GPNMB/Osteoactivin extracellular domain with angiogenic properties. PLoS One *5*, e12093. https://doi.org/10.1371/journal.pone.0012093.
77. Brendza, R., Lin, H., Stark, K., Foreman, O., Tao, J., Pierce, A., Ngu, H., Shen, K., Easton, A.E., Bhangale, T., et al. (2021). Genetic ablation of Gpnmb does not alter synuclein-related pathology. Neurobiol. Dis. *159*, 105494. https://doi.org/10.1016/j.nbd.2021.105494.
78. Pesamaa, I., Muller, S.A., Robinson, S., Darcher, A., Paquet, D., Zetterberg, H., Lichtenthaler, S.F., and Haass, C. (2023). A microglial activity state biomarker panel differentiates FTD-granulin and Alzheimer's disease patients from controls. Mol. Neurodegener. *18*, 70. https://doi.org/10.1186/s13024-023-00657-w.
79. Neal, M.L., Boyle, A.M., Budge, K.M., Safadi, F.F., and Richardson, J.R. (2018). The glycoprotein GPNMB attenuates astrocyte inflammatory responses through the CD44 receptor. J. Neuroinflammation *15*, 73. https://doi.org/10.1186/s12974-018-1100-1.
80. Michell, D.L., and Vickers, K.C. (2016). Lipoprotein carriers of microRNAs. Biochim. Biophys. Acta *1861*, 2069–2074. https://doi.org/10.1016/j.bbalip.2016.01.011.
81. Manelli, A.M., Bulfinch, L.C., Sullivan, P.M., and LaDu, M.J. (2007). Abeta42 neurotoxicity in primary co-cultures: effect of apoE isoform and Abeta conformation. Neurobiol. Aging *28*, 1139–1147. https://doi.org/10.1016/j.neurobiolaging.2006.05.024.
82. Lv, S., Zhang, Y., Lin, Y., Fang, W., Wang, Y., Li, Z., Lin, A., Dai, X., Ye, Q., Zhang, J., and Chen, X. (2023). ApoE4 exacerbates the senescence of hippocampal neurons and spatial cognitive impairment by downregulating acetyl-CoA level. Aging Cell *22*, e13932. https://doi.org/10.1111/acel.13932.
83. Nelson, T.J., and Sen, A. (2019). Apolipoprotein E particle size is increased in Alzheimer's disease. Alzheimers Dement. *11*, 10–18. https://doi.org/10.1016/j.dadm.2018.10.005.
84. Wang, C., Najm, R., Xu, Q., Jeong, D.E., Walker, D., Balestra, M.E., Yoon, S.Y., Yuan, H., Li, G., Miller, Z.A., et al. (2018). Gain of toxic apolipoprotein E4 effects in human iPSC-derived neurons is ameliorated by a small-molecule structure corrector. Nat. Med. *24*, 647–657. https://doi.org/10.1038/s41591-018-0004-z.
85. Fernandez, C.G., Hamby, M.E., McReynolds, M.L., and Ray, W.J. (2019). The Role of APOE4 in Disrupting the Homeostatic Functions of Astrocytes and Microglia in Aging and Alzheimer's Disease. Front. Aging Neurosci. *11*, 14. https://doi.org/10.3389/fnagi.2019.00014.
86. Chen, X., Quinn, E.M., Ni, H., Wang, J., Blankson, S., Redmond, H.P., Wang, J.H., and Feng, X. (2012). B7-H3 participates in the development of experimental pneumococcal meningitis by augmentation of the inflammatory response via a TLR2-dependent mechanism. J. Immunol. *189*, 347–355. https://doi.org/10.4049/jimmunol.1103715.
87. Schildge, S., Bohrer, C., Beck, K., and Schachtrup, C. (2013). Isolation and culture of mouse cortical astrocytes. J. Vis. Exp. 50079. https://doi.org/10.3791/50079.
88. Morikawa, M., Fryer, J.D., Sullivan, P.M., Christopher, E.A., Wahrle, S.E., DeMattos, R.B., O'Dell, M.A., Fagan, A.M., Lashuel, H.A., Walz, T., et al. (2005). Production and characterization of astrocyte-derived human apolipoprotein E isoforms from immortalized astrocytes and their interactions with amyloid-beta. Neurobiol. Dis. *19*, 66–76. https://doi.org/10.1016/j.nbd.2004.11.005.
89. DeMattos, R.B., Curtiss, L.K., and Williams, D.L. (1998). A minimally lipidated form of cell-derived apolipoprotein E exhibits isoform-specific stimulation of neurite outgrowth in the absence of exogenous lipids or lipoproteins. J. Biol. Chem. *273*, 4206–4212. https://doi.org/10.1074/jbc.273.7.4206.
90. Kim, D., Paggi, J.M., Park, C., Bennett, C., and Salzberg, S.L. (2019). Graph-based genome alignment and genotyping with HISAT2 and HISAT-genotype. Nat. Biotechnol. *37*, 907–915. https://doi.org/10.1038/s41587-019-0201-4.
91. Liao, Y., Smyth, G.K., and Shi, W. (2014). featureCounts: an efficient general purpose program for assigning sequence reads to genomic features. Bioinformatics *30*, 923–930. https://doi.org/10.1093/bioinformatics/btt656.
92. Love, M.I., Huber, W., and Anders, S. (2014). Moderated estimation of fold change and dispersion for RNA-seq data with DESeq2. Genome Biol. *15*, 550. https://doi.org/10.1186/s13059-014-0550-8.
93. Zhang, H., Sathyamurthy, A., Liu, F., Li, L., Zhang, L., Dong, Z., Cui, W., Sun, X., Zhao, K., Wang, H., et al. (2019). Agrin-Lrp4-Ror2 signaling regulates adult hippocampal neurogenesis in mice. Elife *8*, e45303. https://doi.org/10.7554/eLife.45303.
94. Pemberton, K., Mersman, B., and Xu, F. (2018). Using ImageJ to Assess Neurite Outgrowth in Mammalian Cell Cultures: Research Data Quantification Exercises in Undergraduate Neuroscience Lab. J. Undergrad. Neurosci. Educ. *16*, A186–A194.

STAR★METHODS

KEY RESOURCES TABLE

REAGENT or RESOURCE	SOURCE	IDENTIFIER
Antibodies		
Anti-mouse apoE	Cell Signaling Technology	Cat#68587; RRID: AB_3094528
Anti-mouse PSD95	Millipore	Cat#MAB1596; RRID:AB_2092365
Anti-mouse Synaptophysin	Abcam	Cat#ab16659; RRID:AB_443419
Anti-mouse MAP2	Abcam	Cat#ab5392; RRID:AB_2138153
Anti-mouse Histone H3 (tri methyl K27)	Abcam	Cat#ab6002; RRID:AB_305237
Anti-mouse Phospho-Histone H2A.X (Ser139) (20E3)	Cell Signaling Technology	Cat#9718; RRID: AB_2118009
Anti-mouse GPNMB	Cell Signaling Technology	Cat#90205
Anti-mouse apoE	Santa Cruz	Cat# sc-6384; RRID:AB_634036
Anti-mouse apoE	Creative Biolabs	Cat#TAB-0974CLV
Anti-human ApoE	Meridian Life Science	Cat# K74180B; RRID:AB_150544
Anti-human ApoE	Invitrogen	Cat# 701241; RRID:AB_2532438
Anti-mouse Iba1	Novus Biologicals	Cat# NB 100–1028; RRID:AB_521594
Anti-mouse GFAP	Cell Signaling Technology	Cat# 3670; RRID:AB_561049
Anti-mouse Neun	Abcam	Cat# ab177487; RRID:AB_2532109
6 nm Colloidal Gold-AffiniPure Goat Anti-Rabbit IgG(H + L)	Jackson	Cat#111-195-144
Chemicals, peptides, and recombinant proteins		
Osteoactivin/GPNMB	SinoBiological	Cat#50475-M088H
Murine GM-CSF	peprotech	Cat#315-03
Critical commercial assays		
Mouse Apolipoprotein E ELISA Kit	Abcam	Cat#ab215086
Lipid removal agent (LRA)	Millipore Sigma	Cat#13358-U
Deposited data		
RNA-seq	This paper	Database: GSE246888
AD related database	This paper	Database: GSE44772
Experimental models: Organisms/strains		
Mouse: C57BL/6J	Xiamen University and Chongqing Medical University	N/A
Mouse: 5 xFAD transgenic mice	The Jackson Laboratory	RRID:MMRRC_034840-JAX
Mouse: GPNMB KO	Cyagen	KOCMP-93695
Mouse: APOE3-TR mouse, 1548	Taconic Bioscience	N/A
Mouse: APOE4-TR mouse, 1549	Taconic Bioscience	N/A
Oligonucleotides		
Primers for Q-RT PCR, see Table S1	This paper	N/A

(*Continued on next page*)

Continued

REAGENT or RESOURCE	SOURCE	IDENTIFIER
Software and algorithms		
Fiji	NIH	https://imagej.net/Fiji
GraphPad Prism	GraphPad	https://www.graphpad.com/scientific-software/prism/
Imaris	OXFORD INSTRUMENTS	Microscopy Image Analysis Software - Imaris - Oxford Instruments (oxinst.com)
The Database for Annotation, Visualization and Integrated Discovery (DAVID) v6.8	https://david.ncifcrf.gov/	DAVID Functional Annotation Bioinformatics Microarray Analysis (ncifcrf.gov)

RESOURCE AVAILABILITY

Lead contact

Further information and requests for resources and reagents should be directed to and will be fulfilled by the lead contact, Yingjun Zhao (yjzhao@xmu.edu.cn).

Materials availability

This study did not generate new unique materials.

Data and code availability

- Bulk RNA-seq data have been deposited at GEO and are available as of the date of publication. Accession number is GSE246888 (as listed in the key resources table). This paper analyzes existing, publicly available data. The accession numbers for these datasets are listed in the key resources table.
- This paper does not report original code.
- Any additional information required to reanalyze the data reported in this paper is available from the lead contact upon request.

EXPERIMENTAL MODEL AND SUBJECT DETAILS

Mice

C57BL/6J WT mice were obtained from the Laboratory Animal Center at Xiamen University and Chongqing Medical University. *APOE3* and *APOE4* targeted replacement mice, which express human apoE isoforms driven by the endogenous murine *Apoe* promoter, were purchased from Taconic. 5xFAD transgenic mice (B6SJL-Tg (APPSwFlLon, PSEN1*M146L*L286V) 6799Vas/Mmja) were purchased from The Jackson Laboratory (MMRRC stock #34 840-JAX),[43] which express human APP and PSEN1 transgenes with five AD linked mutations (the Swedish [K670N/M671L], Florida [I716V], and London [V717I] mutation in APP, and theM146L and L286V mutation in PSEN1) under the mouse Thy1 promoter. 5xFAD mice were maintained as hemizygotes on a C57BL/6 background. *Gpnmb*-KO mice were purchased from Cyagen (KOCMP-93695-*Gpnmb*-B6J-VA). The mice were maintained at a constant temperature with an alternating 12 h light/dark cycle. Food and water were available *ad libitum*.

Primary cell culture

Brain tissues from C57BL6 mice were dissected for primary glial cell culture. With modification, primary microglial cells were prepared as described.[86] Briefly, mixed glial cells from newborn (postnatal 1 to 3-day-old, mixed sex of male and female) pups were cultured in DMEM (GIBCO) supplemented with 10% FBS and 100 U/mL penicillin/streptomycin in a poly-D-lysine (25 μg/mL) (Sigma)-coated cell culture flasks (Corning, Fisher, USA). The medium was changed within the next day with fresh DMEM medium plus 10% FBS and 12.5 ng/mL GM-CSF (Peprotech). Microglial cells were harvested by shaking at a speed of 220 rpm for 15 min after 9–10 days of culture. The harvested cells were seeded for further experiments.

Primary astrocytes were prepared as described by a previous protocol[87] with modification. Simply, mixed glial cells from newborn (postnatal 1 to 3-day-old) pups were cultured in astrocyte culture media (DMEM, high glucose +10% heat-inactivated fetal bovine serum +1% penicillin/streptomycin). The medium was changed 2 days after the plating of the mixed cortical cells and every 3 days thereafter. On day 9 or day 10, when astrocytes were confluent, mixed cells were shaken at 220 rpm for 30 min to remove the upper microglial cells. Trypsin (Sigma, T2601) was used to split attached astrocytes for further culture or use.

Primary cortical neurons were obtained from 11 to 17 days old embryos of WT C57BL/6 mice and cultured in neurobasal medium (GIBCO) supplemented with 0.5 mM GlutaMAX (GIBCO), 2% B27 (GIBCO), and 1% penicillin-streptomycin (Invitrogen) on cover glasses pre-coated with poly-D-lysine solution (50 μg/mL). At day 5 of the *in vitro* study (DIV5), the neurons were treated with 10 M cytosine arabinofuranoside

(Sigma Aldrich) for 2 days to remove glial cells. At DIV7 the culture medium was then replaced with fresh neurobasal medium containing B27 and penicillin-streptomycin. For neuron-microglia co-cultures, microglia were re-suspended in neuronal culture medium and were seeded on top of primary neurons at DIV8 to a final ratio of 1:2 (microglia: neuron).

Study approval

All animal experiments were approved by the Animal Ethics Committee of Xiamen University and Chongqing Medical University and were conducted in compliance with all relevant ethical regulations for animal testing and research.

METHOD DETAILS

ApoE/lipoprotein particles purification

Both astrocyte and microglia culture medium were replaced with serum-free media (DMEM, high glucose+1% penicillin/streptomycin) 72 h before collection. Media was collected and centrifuged at 1000 g for 5 min to remove cell debris. The supernatant was filtered through a 0.2 μm PVDF filter and then concentrated by Amicon Ultra 10K (Millipore). ApoE/lipoprotein particles were then purified from concentrated culture media by immunoaffinity column.[37,88,89] The immunoaffinity column was prepared by coupling CNBr-activated Sepharose beads (Cytiva) with an anti-mouse apoE antibody (Cat# TAB-0974CLV, Creative Biolabs). Concentrated media was applied to the column and run overnight at 4°C. The immunoaffinity column was washed with 3M NaSCN to elute apoE particles. ApoE particles were dialyzed overnight in PBS with 3 changes at 4°C and concentrated by Amicon Ultra 10K, followed by a concentration of 6 μg/mL were used to treat neurons.

ApoE ELISA

ApoE protein concentration of apoE particles was determined by mouse apoE ELISA Kit (Abcam, Ab215086), following the manufacturer's instructions.

Fast protein liquid chromatography

Conditioned media were generated by culturing cells in serum-free media for 24 h in T75 flasks and then collected. Astrocyte and microglia conditioned media were then concentrated 20-fold using a 10-kDa cut-off filter (Millipore) and centrifuged to remove cellular debris before storage at 4°C prior to fractionation. Samples were run through an AKTA Fast protein liquid chromatography (FPLC) system through a Heparin column (heparin affinity chromatography) or a Superose 6 column (SEC; GE Healthcare). The fractions were blotted onto a nitrocellulose membrane, stained with anti-apoE antibody (Santa Cruz M-20, Cat # sc-6384, Host: Goat) and corresponding secondary antibody for further analysis.

Dynamic light scattering

Purified apoE particles were diluted in filtered PBS and loaded to a cuvette. The measurements were carried out at 25°C with the refractive index of water on Malvern Zetasizer. For each sample, three analysis duplicates were done with 12 runs and each run lasting 10 s. The size distribution of apoE particles was displayed by the detected number.

Electron microscopy and immunoelectron microscopy

Carbon-coated grids were hydrophilized by glow discharge at low pressure in the air. Purified apoE particles were diluted in filtered PBS and loaded onto grids for 5 min. Residual particles were absorbed by filter paper. Samples were negative-stained with uranyl acetate for 5 min. For ImmunoElectron microscopy, colloidal gold was labeled to apoE particles. Briefly, apoE particles were loaded onto hydrophilic grids for 5 min. Instead of BSA, recombinant Goat IgG protein was diluted in PBS and used to block the grids. ApoE particles absorbed grids were incubated with Rabbit apoE antibody (Cat# 68587, CST) for 40 min and then incubated with 6 nm Colloidal Gold AffiniPure Goat Anti-Rabbit IgG (H + L) (Jackson) for 20 min. Finally, the sample was immobilized with 2.5% glutaraldehyde solution for 12 min and negative-stained with uranyl acetate for 5 min. Grids were imaged with an HT7800 transmission electron microscope operating at 80 kV.

Immunofluorescence staining

Cells were fixed in 4% paraformaldehyde and then permeabilized with 0.25% Triton X-100 in PBS. After blocking with 10% donkey serum in PBST for 1 h, cells were incubated with primary antibody overnight at 4°C. After washing with PBS, cells were incubated with Alexa-conjugated secondary antibody for 1 h at room temperature. The nuclei were labeled with DAPI (Abcam, ab104139). Fluorescent signals were detected by confocal laser scanning fluorescent microscopy (LSM980, Zeiss). Primary antibodies used for immunostaining include: MAP2 (Chicken, 1:500, Abcam, ab5392); PSD95 (Mouse, 1:100, Neuromab, 75-028); SYP (Rabbit, 1:200; Abcam, ab16659); γH2AX (Rabbit, 1:500, CST, 9718); H3K27me3 (Rabbit, 1:500, Abcam, ab6002).

Immunohistochemistry staining

Mouse brain sections were washed in PBS for 3 times, 5 min each. After washing, sections were permeabilized/blocked in 5% BSA/0.1% TBS-T (Triton X-100)- for 1 h, followed by 3 times washes in TBS. Then brain sections were incubated with primary antibodies (Neun antibody, Abcam

ab177487; GFAP antibody, CST 3670; Iba1 antibody, Novus Biologicals B 100–1028) at 4°C for overnight. The next day, after 3 times washes in TBS, sections were incubated with corresponding fluorescence-labeled secondary antibodies for 1.5 h at room temperature. The sections were then washed and mounted in Antifade Mounting Medium (Solarbio S2100). Fluorescent signals were detected by spinning disk confocal super resolution microscope (Olympus SpinSR10).

RNA extraction and quantitative RT-PCR

Total RNA from cell was extracted using Monarch Total RNA Miniprep Kit (NEB), following the manufacturer's instructions. Total RNA quantity was measuring using the Nanodrop2000 (Thermofisher). Total RNA (2 μg) was reverse-transcribed to cDNA using FastKing RT Kit (TIANGEN). qPCR reactions were performed using SYBR green (Abclonal) on the Light Cycler 480 System (Roche). Relative expression was determined using the comparative Ct model (ΔΔCt) with glyceraldehyde 3-phosphate dehydrogenase (Gapdh) as a reference. Primers for individual genes can be found in Table S1.

Western Blot

ApoE particles were mixed with 6×Protein Loading Buffer and then incubated at 95°C for 5 min. Astrocytic and microglial apoE particles including equal amounts of apoE protein were loaded into 10% SDS-PAGE and separated by electrophoresis. Proteins were then transferred from gel to 0.45 μm PVDF membrane. Membranes were blocked with 5% non-fat milk and then incubated with primary antibody at 4°C overnight, followed by secondary antibody incubation. Immuno-reactive bands were visualized by Chemiluminescent HRP Substrate (Millipore), detected by ChemiScope (CLINX), and quantified by ImageJ software.

Delipidation

To verify GPNMB is one component of microglial apoE particles, particles were delipidated using Lipid removal agent (LRA) (sigma 13358-U). Briefly, 100 μg of LRA (from 100 mg/mL stock solution in 50 mM ammonium bicarbonate) per 1 μg of microglial apoE particles were mixed gently in 300 μL PBS and rotated for 1 h at room temperature. Then the LRA was centrifuged by centrifugation (2200 × g for 2 min) and the supernatant was collected. The pellet was added 20 μL 50 mM ammonium bicarbonate premixed with 6× SDS-PAGE loading buffer (ABclonal RM0001) and heat for 5 min at 95°C. The supernatant was also mixed with 6× SDS-PAGE loading buffer and heat for 5 min at 95°C for further analysis.

Electrophysiological recording

Whole-cell voltage-clamp recordings were performed on mice embryonic cortical neurons maintained in culture for DIV 12. The patch pipettes were pulled from borosilicate glass capillary tubes (Sutter, Cat# BF150-86-10) using a Model P-1000 (Sutter). The resistance of pipettes filled with intracellular solution varied between 5 and 8 MΩ. Synaptic currents were monitored with a Multiclamp 700B amplifier (Molecular Devices) and synchronized with Clampex 10.6 data acquisition software (Molecular Devices). A whole-cell pipette solution was used containing (in mM) 140 mM CsCH3SO3, 2 mM MgCl2 6H2O, 5 mM TEA-Cl, 10 mM HEPES, 1 mM EGTA, 2.5 mM Mg-ATP, and 0.3 mM Na-GTP (pH 7.3, 300 mOsm). The external bath solution contained (in mM) 2.5 mM KCl, 126 mM NaCl, 2.4 mM MgCl2, 1.2 mM CaCl2, 1.2 mM NaH2PO4, 11 mM glucose, and 18 mM NaHCO3 (pH 7.4, 300 mOsm). mEPSCs recordings was performed while holding the cell at −70 mV mEPSCs was monitored in the presence of tetrodotoxin (1 μM) (Fisher Cat#507532807) to block action potentials. All recordings were performed at RT. Cells with a series resistance of >30 MU throughout the recording were excluded from the analysis. Synaptic currents were filtered at 0.5 kHz, sampled at 10 kHz and analyzed offline using Clampfit 9 (Molecular Devices) software.

RNA sequencing analysis

RNA was isolated from primary neurons treated with astrocytic or microglial apoE particles and subjected to RNA-seq analysis. cDNA library construction and sequencing were performed by the BGI using BGI platform. Sample quality was assessed by FastQC (https://www.bioinformatics.babraham.ac.uk/projects/fastqc). Samples were aligned to the mouse reference genome GRCm38 using HISAT2.[90] Mapped sequencing reads were assigned to genomic features with the featureCounts function.[91] DESeq2[92] was used to identify DEGs between samples. Genes were considered differentially expressed if the adjusted p-value was lower than 0.05 and the absolute value of fold change was greater than 2. KEGG enrichment was performed using the richR package (https://github.com/hurlab/richR) and an adjusted p-value <0.05 was chosen as the cutoff value to select significant KEGG pathways.

ApoE particle injection

Female 5xFAD mice aged 5 months were anesthetized with isoflurane. ApoE particles (1 μL, 1 μg/μL) were stereotaxically injected into the bilateral hippocampus (bregma, −2.5 mm; lateral, ±2.0 mm; depth, −2.0 mm) of the mouse using a syringe (Hamilton; syringe 7635-01 and needle 7762-05). Behavioral tests were conducted 7 days after the injection.

Morris Water Maze

The MWM was used to measure acquisition and expression of spatial memory as previously described.[93] A circular water tank (120 cm diameter and 40 cm height) was filled with water (22°C, 25 cm deep) and in the presence of a constellation of spatial cues visible to the mice.

Nontoxic white powder paint was added to the water to make the surface opaque and to hide the escape platform (circular platform, 6 cm in diameter, 1 cm below the surface). The experimental protocol required five days of acquisition with the platform in place (four trials per day) and removal of the platform on the sixth day for a probe test. During the acquisition phase, the platform stayed in the same location for each animal. At the beginning of each trial, the mice were placed into one of the four quadrants facing the wall and the starting location varied pseudo randomly across trials for each mouse. Mice were given 60 s to find the platform, at which point the experimenter would guide the animal to the platform if necessary. Mice remained on the platform for 30 s, and were then dried with a towel and placed under a 37°C lamp between trials. To measure the rate of acquisition, the latency to reach the platform was averaged over all four trials each day. For the probe trial, mice were given 60 s to swim and the trajectory and amount of time spent in each quadrant was recorded and analyzed by CleverSys TopSanLite (Clever Sys, Reston, VA, USA).

Mass spectrometry

Samples were subjected to in-gel trypsin digestion and dried, followed by analysis using an EASY-nLC 1200 (Thermo SCIENTIFIC) coupled to an Orbitrap Fusion Lumos (Thermo SCIENTIFIC) equipped with an EASY-IC ion source. Peptides were dissolved in 10 μL 0.1% formic acid and directly auto-sampled onto a homemade C18 column (35 cm × 75 μm i.d., 2.5 μm 100 Å). Elution was performed over 120 min using linear gradients of 3–35% acetonitrile in 0.1% formic acid at a flow rate of 300 nL/min. The raw files obtained from the analysis were processed using Proteome Discoverer 2.2 software, matching the identified peptides against Uniprot database. Only proteins with #Peptides >10 and #Unique Identifications >10 were included in the UpSet graph.

Analysis of apolipoprotein E gene particle sizes by native PAGE

The medium of primary microglial culture was replaced with serum-free medium 48 h before medium collection. Then the conditioned medium was harvested and concentrated. Avidin-agarose beads (Pierce) were pre-coupled with biotinylated polyclonal anti-APOE antibody (K74180B, Meridian Life Science) and then incubated overnight with concentrated conditioned media at 4°C. Complexes of bead-antibody-apoE were washed with TBS buffer three times, 0.1 M glycine (pH 2.5) was used to elute immunoprecipitated apoE and then neutralized with 1 M Tris (pH 8.5). Particles containing equal amounts of APOE3 or APOE4 proteins were subjected to native electrophoresis using Native PAGE Novex 4–20% Tris-Glycine gels (Thermo Fisher) followed by immunoblot with goat anti-apoE antibody (K74180B, Meridian Life Science).

QUANTIFICATION AND STATISTICAL ANALYSIS

For primary neuronal experiments, 6–10 cells from each group, and data from 3 to 5 independent experiments were analyzed and quantified following a method reported previously.[94] Neurite number (neurite initiation sites) and length were counted and measured using ImageJ. Data are present as mean ± standard error of the mean (SEM). For two independent data comparisons, unpaired Student's t test was used to determine statistical significance. For multiple comparisons, one-way or two-way ANOVA test were used to determine statistical significance. No statistical analysis was used to determine sample size prior. The sample sizes chosen are based on our previous studies from our laboratory. The number of samples indicates biological replicates as indicated in each of the figure legends. *, $p < 0.05$; **, $p < 0.01$; ***, $p < 0.001$. Statistical analyses were performed using Excel 2019 (Microsoft) or GraphPad Prism9.0.